Eur. Phys. J. C (2024) 84:1116
https://doi.org/10.1140/epjc/s10052-024-13453-7

THE EUROPEAN PHYSICAL JOURNAL C

Regular Article - Theoretical Physics

Electron-positron pair creation under Gaussian and super-Gaussian pulse trains

X. X. Zhou[1,a], **X. N. Cao**[1], **C. K. Li**[2], **N. S. Lin**[3], **Y. J. Li**[3,4,b]

[1] School of Management Science and Engineering, Anhui University of Finance and Economics, Bengbu 233030, Anhui, China
[2] Laboratory of Zhongyuan Light, School of Physics, Zhengzhou University, Zhengzhou 450001, China
[3] School of Science, China University of Mining and Technology, Beijing 100083, China
[4] State Key Laboratory for Geomechanics and Deep Underground Engineering, China University of Mining and Technology, Beijing 100083, China

Received: 27 May 2024 / Accepted: 26 September 2024

Abstract The electron-positron pair (EPP) creation under Gaussian and super-Gaussian pulse trains are studied by the computational quantum field theory (CQFT) in the single-photon regime. The details of the EPP creation are studied from the time evolution of the EPP number, energy spectra and spatial distribution of the electrons. The results indicate that the final created EPPs is the non-linear accumulation of the multi-pulses, which depends on the time interval, pulse shape and pulse number. The optimal time interval can be chosen based on the pulse resonance condition, which is derived by the perturbation method. Besides, steeper super-Gaussian pulses and adding more pulses facilitate the EPP creation as well. The results indicate that, under optimal multi-pulse parameters, the number of the EPPs obtained is much larger than the sum of the EPPs created under the same number of single pulses. This finding not only can enhance the EPP creation, but also can improve the multi-pulse utilization and guide future experimental research on the EPP creation.

1 Introduction

One of the most astonishing theoretical predictions of quantum electrodynamics (QED) is that the electron-positron pairs (EPPs) can be created from the vacuum under the strong external field. In 1951, Schwinger calculated the EPP creation rate $P_{e^+e^-} \sim exp(-\pi E_{cr}/E)$ under ultra-strong uniform electrostatic field, in which the critical electric field strength $E_{cr} = 1.3\times10^{18}\ V/m$ [1]. E_{cr} requires a laser intensity of up to $10^{29}\ W/cm^2$, whereas the current laser intensity that can be achieved is about $10^{23}\ W/cm^2$ [2]. Therefore, the Schwinger mechanism cannot be directly verified experimentally nowadays. The EPPs can also be created by the time-dependent field. With the development of the laser technology, ultra-short and ultra-strong laser pulses have been widely applied to the creation of the EPPs [3–5].

The researches on the EPP creation under time-dependent fields mainly involves the single short laser pulses, and the combination of short pulses, etc. Previous researches indicated that the EPP creation depends sensitively on the pulse shape, pulse intensity, pulse duration and the carrier envelope phase, etc [6–11]. Moreover, the pulse combination can bring some new effects that promote the EPP creation, e.g., the dynamically assisted Schwinger effect occurring in the combination of strong and slow pulse with weak and fast pulse can significantly enhance the EPP creation [12–14], and the EPP creation under the double-pulse with time-interval can be significantly enhanced by choosing proper time interval [15–17]. If the field is composed by multi-pulses with time interval (i.e. pulse train), what phenomenon will occur in the EPP creation?

In recent years, efforts have been concentrated on the generation of pulse trains due to its increasing applications in fundamental sciences and advanced technologies [18,19]. For instance, pulse trains have been extensively applied to the control of photon transition dynamics in atomic or molecular systems. Among them, the occurrence of pulse coherence or pulse resonance effects can lead to interesting phenomena, such as population accumulation and resonance transitions in atomic systems under weak optical excitation [20,21]. The pulse train is characterized by pulse parameters (i.e. pulse strength, pulse shape, pulse duration, time interval etc.), and the parameterization allows for systematic and convenient

[a] e-mail: xxzhouphys@163.com (corresponding author)
[b] e-mail: lyj@aphy.iphy.ac.cn

Published online: 28 October 2024

control of the corresponding researches. This makes pulse trains into a popular tool. It may be possible to experimentally observe the creation of the EPPs from the vacuum through pulse train in the future, and the relevant theoretical research on the EPP creation is necessary. There were some studies on the pair creation under multi-pulse field, e.g., the alternating-sign N-pulse configuration for spinor QED was studied and additionally the configurations consisting of equal-sign pulses was examined [24], the boson pair creation in an alternating-sign N-pulse electric field was investigated [23], and the creation of the EPPs induced by the field composed of two sets of alternating-sign N-pulse fields was investigated. Previous studies have shown many interesting phenomena of the EPP creation under multi-pulse field [22]. Even so, further researches are needed on the creation of the EPPs under multi-pulse field: previous researches mainly focused on alternating-sign multi-pulse field, while there was little research on equal-sign multi-pulse field; the external field only has a temporal distribution, and the spatial distribution was simply considered uniform; finally, previous studies have mainly focused on the momentum spectra, while there was little research on the temporal evolution and spatial distribution of the created EPPs. In our work, the EPP creation under the equal-sign multi-pulse field is studied, of which the spatial distribution follows Sauter potential. We systematically study the details of EPP creation, including the temporal evolution of EPP number, energy spectra, and spatial distribution. Besides, the effects of the pulse time interval, pulse number, and pulse steepness on the EPP creation are studied, as well as the optimal creation conditions.

The paper is organized as follows. In Sect. 2, we introduce the computational quantum field theory (CQFT) that permits us to calculate the spatio-temporal pair creation probability for arbitrary external force field. In Sect. 3, the EPP creation under the equal-sign multi-pulse field is studied, and we analyse the effects of the time interval, the pulse duration, the pulse number, and the pulse shape on the EPP creation. In Sect. 4, we give the conclusion and outlook.

2 The theoretical method

The computational quantum field theory (CQFT) is applied to study the EPP creation process. The time evolution of the quantum field operator $\hat{\psi}(x,t)$ is described by the Dirac equation [25–29] (*Here and below we use atomic unit*).

$$i\frac{\partial}{\partial t}\hat{\psi}(x,t)=\left[c\sigma_1 p_x+\sigma_3 c^2+V(x,t)\right]\hat{\psi}(x,t), \tag{1}$$

where σ_1 and σ_3 are the Pauli matrices. The electric field is described by the scalar potential $V(x,t)$. We focus on the x axis, and the Dirac four component spinor wave functions can be reduced to two components [28,29].

Notably, the field operator not only satisfies the Dirac equation, but also satisfies the time-dependent Heisenberg equation $i\partial\hat{\psi}(t)/\partial t = [\hat{H},\hat{\psi}(t)]$ [29–31]. The quantum field theoretical Hamiltonian $\hat{H} = \hat{\psi}^{\dagger}h\psi$, where $h = h_0 + V(x,t)$. $h_0 = c\sigma_1 p_x + \sigma_3 c^2$ is the field-free Hamiltonian. The field operator can be expanded by the particle annihilation operator ($\hat{b}_p$) and the antiparticle creation operator ($\hat{d}_n^{\dagger}$)

$$\begin{aligned}\hat{\psi}(x,t)&=\sum_p \hat{b}_p(t)u_p(x)+\sum_n \hat{d}_n^{\dagger}(t)v_n(x)\\&=\sum_p \hat{b}_p u_p(x,t)+\sum_n \hat{d}_n^{\dagger}v_n(x,t),\end{aligned} \tag{2}$$

$u_p(x)$ ($E \geq c^2$) and $v_n(x)$ ($E \leq -c^2$) are the energy eigenstates of h_0. $u_p(x,t)$ and $v_n(x,t)$ satisfies the Dirac equation [Eq. (1)]. The subscripts p and n represent the positive and negative energy, respectively. The time evolution of the fermion annihilation and creation operators are

$$\begin{aligned}\hat{b}_p(t)=&\sum_{p'}\hat{b}_{p'}\int dx u_p^*(x)u_{p'}(x,t)\\&+\sum_{n'}\hat{d}_{n'}^{\dagger}\int dx u_p^*(x)v_{n'}(x,t),\end{aligned} \tag{3}$$

$$\begin{aligned}\hat{d}_n^{\dagger}(t)=&\sum_{p'}\hat{b}_{p'}\int dx v_n^*(x)u_{p'}(x,t)\\&+\sum_{n'}\hat{d}_{n'}^{\dagger}\int dx v_n^*(x)v_{n'}(x,t),\end{aligned} \tag{4}$$

respectively. The electronic portion of the field operator $\hat{\psi}_e(x,t) \equiv \sum_p \hat{b}_p(t)u_p(x)$, the positronic portion of the field operator $\hat{\psi}_{e^+}(x,t) \equiv \sum_n \hat{d}_n^{\dagger}(t)v_n(x)$. Using the commutator relations $[\hat{b}_p,\hat{b}_{p'}^{\dagger}]_+ = \delta_{p,p'}$ $[\hat{d}_n,\hat{d}_{n'}^{\dagger}]_+ = \delta_{n,n'}$, the spatial distribution of the created electrons and positrons are

$$\begin{aligned}\rho_e(x,t)&\equiv\langle\langle \mathrm{vac}\|\hat{\psi}_e^{\dagger}(x,t)\hat{\psi}_e(x,t)\|\mathrm{vac}\rangle\rangle\\&=\sum_{p,n}\left|\langle p|U(t)|n\rangle u_p(x)\right|^2,\end{aligned} \tag{5}$$

$$\begin{aligned}\rho_{e^+}(x,t)&\equiv\langle\langle \mathrm{vac}\|\hat{\psi}_{e^+}^{\dagger}(x,t)\hat{\psi}_{e^+}(x,t)\|\mathrm{vac}\rangle\rangle\\&=\sum_{p,n}|\langle n|U(t)|p\rangle v_n(x)|^2,\end{aligned} \tag{6}$$

where $\|\mathrm{vac}\rangle\rangle$ is the initial vacuum state, the double bars and brackets are used to indicate that this is a state of the second-quantised quantum field theory [29]. The usual quantum mechanical states are denoted by a single bar and bracket.

Finally, the total number of the created EPPs is defined as

$$N(t) = \int dx \rho_e(x,t) = \sum_p \langle\langle \text{vac} \| \hat{b}_p^\dagger(t) \hat{b}_p(t) \| \text{vac} \rangle\rangle = \sum_{p,n} |\langle p|U(t)|n\rangle|^2 . \quad (7)$$

The time evolution operator $U(t) = \hat{T} exp[-i \int_0^t h(t')dt']$ evolves the field-free negative state $|n\rangle$ (*i.e.* $v_n(x, t = 0)$) under Eq. (1) to get the evolved-state $|n(t)\rangle$. The total time evolution from 0 to t_{max} is decomposed into N_T consecutive actions, each time step $\Delta t = t_{max}/N_T$ with an order of $10^{-6} a.u$. Applying the split operator technique [32–34], the time evolution operator in each time step is written as $U(t+\Delta t, t) = exp(\frac{-iV\Delta t}{2}) exp(-ih_0\Delta t) exp(\frac{-iV\Delta t}{2}) + O(\Delta t^3)$, and the error in each step is of order $O(\Delta t^3)$ ensuring the convergence of the numerical calculation. Finally, by using the fast Fourier transformation (FFT) between the spatial and momentum space, the time-evolved state $|n(t)\rangle = U(t)|n\rangle$ can be obtained, and then the spatial and energy distribution, as well as the total EPP number can be calculated out.

The external field represented by the scalar potential is $V(x,t) = V(x)f(t)$, where $f(t)$ is the temporal distribution. $V(x) = V[1 + \tanh((x - x_0)/W)]/2$ is the spatial distribution, which indicates that the electric pulse is confined in a range of about $2W$ along the x direction [35]. The temporal distribution $f(t)$ is composed of several Gaussian pulses, in which each pulse is the same and the time interval between the adjacent pulses is also the same. The expression of $f(t)$ is as follows,

$$f(t) = \sum_{k=1}^{M} e^{-[(t-t_k)^2/2T^2]}, \quad (8)$$

where T is the pulse duration and V is the pulse strength, and in our model the strength and duration of each pulse are the same. M is the number of the pulses that composites the field. $t_k = (2k-1)t_1 + (k-1)\tau$ is the time center of the $k-th$ pulse, where t_1 is the time center of the first pulse, and τ is the time interval between adjacent pulses. The schematic diagram of the temporal distribution of the combined field is shown in Fig. 1.

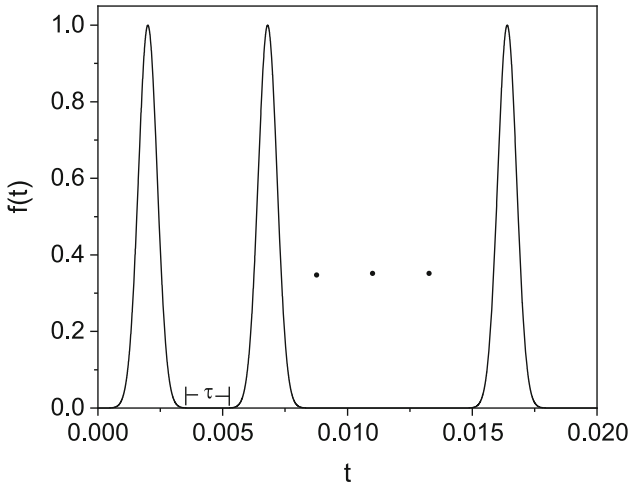

Fig. 1 The schematic diagram of the temporal distribution of the field composed by several Gaussian-pulses

3 Results and discussion

In this section, the creation of the EPPs under equal-sign double and multi-pulse field are studied by CQFT. Firstly, the effects of the time interval and pulse duration on the time evolution of the EPP number are studied in a double-pulse field. The condition that time interval affects the EPP creation is derived by the perturbation method. Then, we extend the field into a multi-pulse field and study the effects of the pulse number and pulse shape on the time evolution of the EPP number. Meanwhile, we compare the relationship between the growth rate of the EPP number and the number of the pulses. Finally, we further investigate the details of the EPP creation under the multi-pulse field from the time evolution of the energy spectra and spatial distribution.

3.1 EPP creation under double-pulse field

In this section, the field composed by two equal-sign Gaussian-pulses (i.e.,$M = 2$) is applied. The time evolution of the total created EPP number under the filed is shown in Fig. 2. Without loss of generality, several time intervals are chosen to study the effects of time interval on the EPP creation. Besides, due to the EPP creation generally depends on pulse duration, two pulse durations are considered as well.

As shown in Fig. 2, the number of the EPPs calculated by CQFT is represented by solid lines, and the time evolution of the EPP number is sensitively depends on the time interval between the two Gaussian-pulses. Three time intervals are chosen: $\tau = 7.75E-5$ (i.e. $\tau = 7.75 \times 10^{-5}$), $1.61E-4$ and $2.4E-4$. The EPP number reaches a certain value when the first pulse is finished, after the time interval τ, the EPP number continue grows under the action of the second pulse. When $T = 1/\sqrt{2}c^2$, there is a significant stepwise increase in the EPP number under the action of the second pulse when $\tau = 7.75E-5$ and $2.4E-4$, and the final EPP number is the accumulation of the sequential action of the two pulses. Moreover, the final EPP number is greater than the sum of the EPPs created by two single pulses acting alone. However, when the time interval $\tau = 1.61E-4$, the EPPs created under the second pulse is very small and negligible, and the

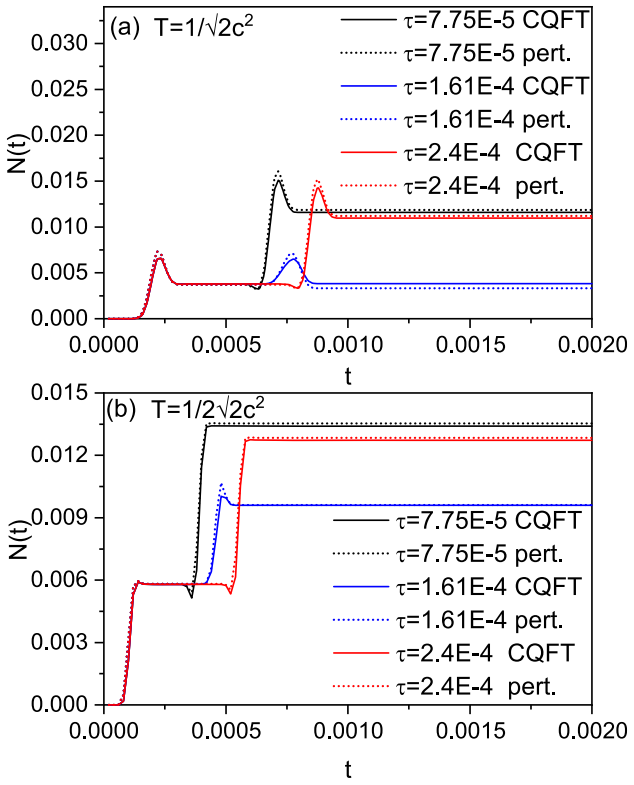

Fig. 2 The time evolution of the total created EPP number under the field composed by two Gaussian-pulses. (**a**) The pulse duration $T = 1/\sqrt{2}c^2$, (**b**) the pulse duration $T = 1/2\sqrt{2}c^2$ The calculation results of CQFT are represented by solid lines, and the results of first-order perturbation method are represented by dashed lines. The first time center $t_1 = 0.000202a.u.$ and $t_1 = 0.000102a.u.$ for $T = 1/\sqrt{2}c^2$ and $T = 1/2\sqrt{2}c^2$, respectively. The other parameters $V = 1.5c^2$,$W = 3/c$, and the final time $t_f = 0.002a.u.$

final EPP number is small as well. When the pulse duration $T = 1/2\sqrt{2}c^2$, the time evolution of the EPP numbers are shown in Fig. 2b. When $\tau = 7.75E-5$ and $2.4E-4$, the number of the EPPs increases greatly under the action of the second pulse, and the final EPP number is very large. When the time interval $\tau = 1.61E-4$, the number of the EPPs created under the second pulse is a little small, but is larger than the EPPs created at $T = 1/\sqrt{2}c^2$ and $\tau = 1.61E-4$. Therefore, under different pulse duration, the accumulation effect occurs in the time evolution of the EPP number, which can be enhanced or weakened by different time intervals. Besides, at the same time interval, the number of the EPPs created changes with pulse duration. By selecting an appropriate time interval, the creation of the EPPs can be significantly promoted. In addition, the time evolution of the EPP number numerically calculated based on the first-order perturbation formula (Eqs. (9, 10)) is represented by dashed lines in Fig. 2. Interestingly, the numerical results computed by the first-order perturbation theory and CQFT are in good agreements, this indicates that the pair creation

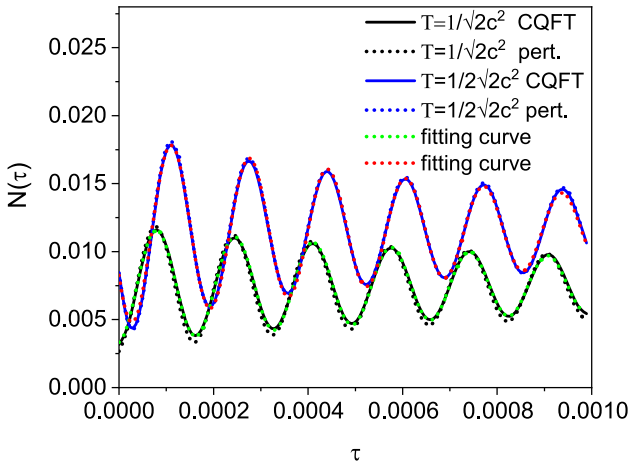

Fig. 3 The dependence of the final EPP number on the time interval under the field composed by two Gaussian-pulses. The black line corresponds to the pulse duration $T = 1/\sqrt{2}c^2$, and the green dashed line is the fitting curve; The blue line corresponds to the pulse duration $T = 1/2\sqrt{2}c^2$, and the red dashed line is the fitting curve. The other parameters $V = 1.5c^2$,$W = 3/c$, and the final time $t_f = 0.003a.u.$

in the single-photon regime. Since there are high frequency Fourier components in the pulse, the electron-positron pairs can be created by absorbing single-photon transitions.

The first-order transition amplitude from the negative state $|n\rangle$ to the positive state $|p\rangle$ at an arbitrary time t is given by

$$\begin{aligned} C_{pn}^{(1)}(t,\tau) &= \frac{1}{i}\int_0^t \langle p|H^{'}|n\rangle e^{i(E_p-E_n)\xi}d\xi \\ &= \frac{1}{i}\int_0^t \langle p|V(x)|n\rangle f(t) e^{i(E_p-E_n)\xi}d\xi \\ &= V_{pn}\int_0^t \{e^{-[\frac{(\xi-t_1)^2}{2T^2}]} + e^{-[\frac{(\xi-t_2)^2}{2T^2}]}\} e^{i(E_p-E_n)\xi}d\xi \end{aligned} \tag{9}$$

Where $V_{pn} = \frac{1}{i}\langle p|V(x)|n\rangle$. By summing over all the states of p and n, we can obtain the first-order perturbation estimation of the total EPP creation as

$$N^{(1)}(t,\tau) = \sum_{p,n}\left|C_{pn}^{(1)}(t,\tau)\right|^2 \tag{10}$$

In order to obtain a more comprehensive understanding of the dependence of the final EPP number (i.e. $t = 0.002a.u.$) on the time interval, we numerically calculate the final EPP number based on CQFT (Eq. (7)) and the first-order perturbation formula (Eq. (10)), respectively.

As shown in Fig. 3, the results based on CQFT and the perturbation formula are represented by solid and dashed lines, respectively, and the two results are in good agreement. The number of the EPPs oscillates with the time interval, alternating between peaks and valleys. The peak of the $N(\tau)$ curves are caused by pulse resonance, which can significantly enhance the EPP creation. To obtain the resonance condition,

we derive the formula for $N(\tau)$ by the first-order perturbation method as follows

$$
\begin{aligned}
N^{(1)}(\tau) &= \sum_{p,n} \left| C_{pn}^{(1)}(t_f, \tau) \right|^2 \\
&= \sum_{p,n} \left| V_{pn} \int_0^{t_f} \{ e^{-[\frac{(\xi - t_1)^2}{2T^2}]} + e^{-[\frac{(\xi - t_2)^2}{2T^2}]} \} e^{i(E_p - E_n)\xi} d\xi \right|^2 \\
&\approx \sum_{p,n} \left| V_{pn} \int_{-\infty}^{\infty} \{ e^{-[\frac{(\xi - t_1)^2}{2T^2}]} + e^{-[\frac{(\xi - t_2)^2}{2T^2}]} \} e^{i(E_p - E_n)\xi} d\xi \right|^2 \\
&= 4\pi T^2 \sum_{p,n} |V_{pn}|^2 e^{-[T^2(E_p - E_n)^2]} [2 + cos[(2t_1 + \tau)(E_p - E_n)],
\end{aligned}
\tag{11}
$$

where t_f is the final time of the numerical simulation. The result of Eq. (11) indicates that the time interval can periodically adjust the final EPP number. The pulse resonance occurs and there is a maximum EPP creation, when the cosine function reaches its maximum value. The resonance condition fulfils $(\tau + 2t_1) \triangle E = 2k\pi (k = 0, 1, 2...)$, where $\Delta E = E_p - E_n$ is the energy gap between the electrons transit from the negative energy state to the positive energy state, and the first pulse center $t_1 = 0.000202 a.u.$ and $0.000102 a.u.$ for pulse duration $T = 1/\sqrt{2}c^2$ and $T = 1/2\sqrt{2}c^2$, respectively. The average value of ΔE (*i.e.* $\overline{\Delta E}$) can be approximated as $2c^2$ [16], then $2t_1\overline{\Delta E}$ are 15.2 (for $T = 1/\sqrt{2}c^2$) and 7.7 (for $T = 1/2\sqrt{2}c^2$). To further verify the resonance condition, we fit the $N(\tau)$ curves obtained by the CQFT with the fitting formula (Eq. (12)). The $N(\tau)$ curves obtained by CQFT and the first perturbation method both conform well to the fitting curve in Fig. 3.

$$
N(\tau) = N \exp(-\beta\tau) \cdot \cos(\omega_N \tau + \phi) + N_{inf}, \tag{12}
$$

here N is the amplitude, β is the decay factor, ω_N is the oscillation frequency, ϕ is the phase of the $N(\tau)$ curve, and N_{inf} is the asymptotic total created pair numbers at the long time limit. When $T = 1/\sqrt{2}c^2$, the fitting parameters are $N = 0.004$ $\beta = 752.9$ $\omega_N = 2.02c^2$ $\phi = 15.8$ and $N_{inf} = 0.0076$. When $T = 1/2\sqrt{2}c^2$, the fitting parameters are $N = 0.007$ $\beta = 995.8$ $\omega_N = 2.02c^2$ $\phi = 8.2$ and $N_{inf} = 0.011$. The resonance condition shown by the fitting formula is $\omega_N \tau + \phi = 2k\pi (k = 0, 1, 2, 3...)$, where ω_N is approximately equal to $2c^2$. Comparing with the resonance condition obtained by the perturbation method, $\omega_N \approx \overline{\Delta E}$, and ϕ with the error of within 6% of $2t_1\overline{\Delta E}$ obtained by the perturbation method. Therefore, we obtain the expression for pulse resonance as $\omega\tau + 2t_1\omega = 2k\pi (k = 0, 1, 2, 3...)$, where $\omega = 2c^2$, and the resonance expression can facilitate us to choose an appropriate pulse time interval. When the time interval between the pulses satisfies the resonance condition, the creation of the EPPs can be significantly enhanced. In the following, we study the effects of pulse number and pulse shape on the EPP creation in the multi-pulse field, the pulse duration is chosen as $T = 1/\sqrt{2}c^2$ without loss of generality.

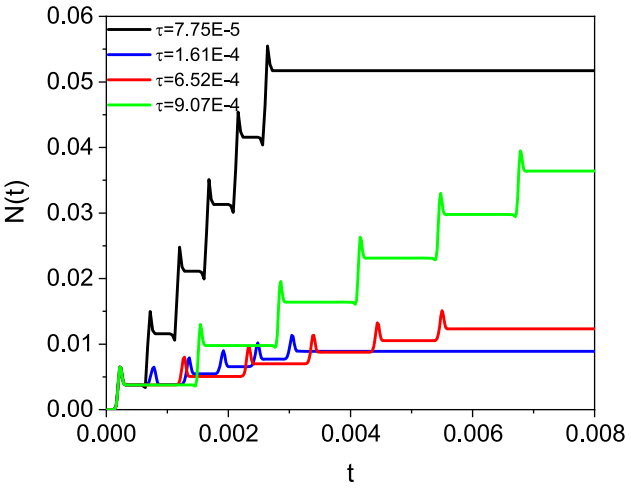

Fig. 4 The time evolution of the EPP number under the field composed of six Gaussian-pulses. Four time intervals are chosen: $\tau = 7.75E-5$ (the black solid line), $\tau = 1.61E-4$ (the blue solid line), $\tau = 6.52E-4$ (the red solid line) and $\tau = 9.07E-4$ (the green solid line). The other parameters $V = 1.5c^2$,$W = 3/c$, the pulse duration $T = 1/\sqrt{2}c^2$, and the final time $t_f = 0.008 a.u.$

3.2 EPP creation under multi-pulse field

When the field composed by two equal-sign Gaussian-pulses, two pulses act in sequence, and the number of the EPPs is the accumulation of the the two pulses. If there are more pulses, the number of the EPPs will be the accumulation of the multi-pulses. Therefore, the final number of the EPPs will increase with the number of the pulses. In the following, the field composed by six pulses, we study the time evolution of the EPP number under four time intervals, which are chosen without loss of generality.

As shown in Fig. 4, the number of the EPPs accumulates under the sequential action of the six Gaussian-pulses. When the time interval is good (e.g. $\tau = 4.1E-4$ and $9.07E-4$), each pulse causes a large EPP creation, and the amount of the EPP growth caused by each pulse is almost the same at the same time interval. When the time interval is poor (e.g. $\tau = 1.61E-4$ and $6.52E-4$), after the first pulse, each pulse causes less EPP creation and ultimately creates fewer final EPPs. Therefore, by increasing the number of the pulses and selecting suitable time interval, the number of the created EPPs can be significantly enhanced.

Subsequently, we study the creation of the EPPs under the field composed by six super-Gaussian pulses, since previous studies on the EPPs created under single pulse concluded that the EPP creation also depends on the pulse shape [10,11]. The temporal distribution of the field is $f(t) =$

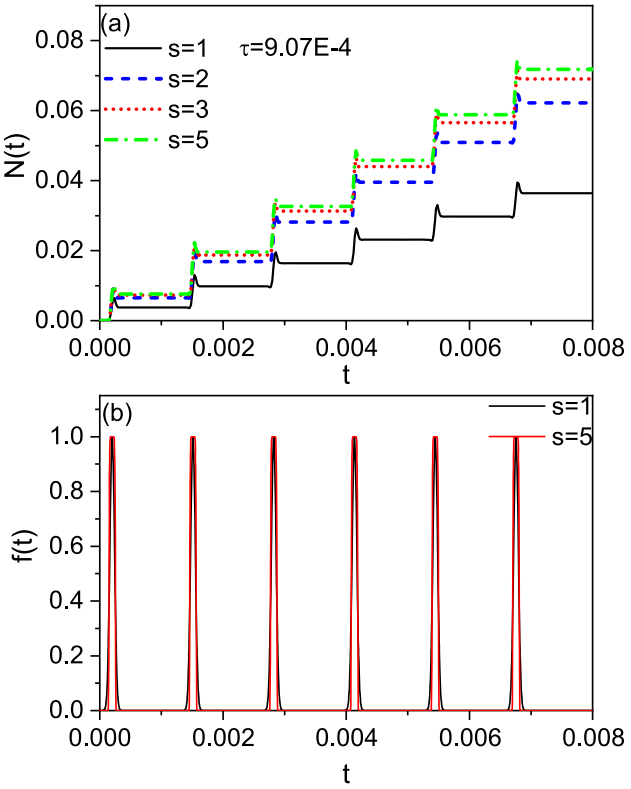

Fig. 5 The time evolution of the EPP number and the pulse shape. (**a**) The time evolution of the EPP number under the field composed of six pulses. Four pulse shapes are chosen: $s = 1$ (the black solid line), $s = 2$ (the blue dash line), $s = 3$ (the red dot line) and $s = 5$ (the green dash dot line). (**b**) The pulse shapes for two different pulse steepness ($s = 1$ and $s = 5$). The other parameters $V = 1.5c^2$,$W = 3/c$, $T = 1/\sqrt{2}c^2$, $\tau = 9.07E - 4$, and $t_f = 0.008a.u.$

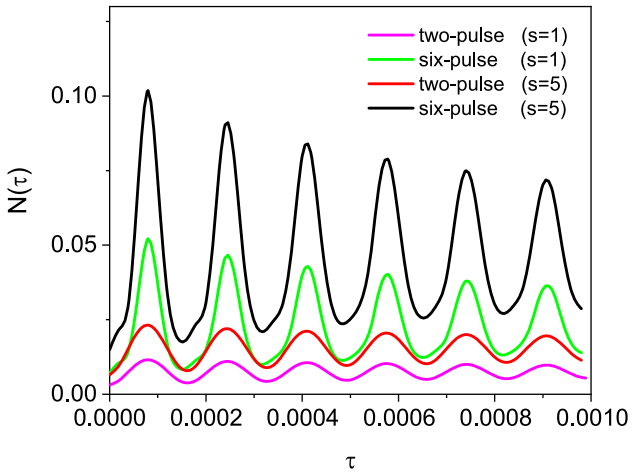

Fig. 6 The dependence of the final EPP number on time interval for field composed by different pulse shapes and pulse numbers. The parameters $V = 1.5c^2$,$W = 3/c$, and the pulse duration $T = 1/\sqrt{2}c^2$

$\sum_{k=1}^{M} e^{-[(t-t_k)^{2s}/2T^{2s}]}$, and the pulse shape can be adjusted by the steepness s. If $s = 1$, the field is composed by Gaussian pulses. If $s > 1$, the field is composed by super-Gaussian pulses. The rising and falling edges of the pulse will become steeper as s increases, and the pulse will approach a rectangular pulse when $s \geq 5$. The schematic diagram of the pulse shape changing with s is shown in the illustration in Fig. 5b.

In Fig. 5, we choose four pulse shapes (i.e. $s = 1$, 2, 3 and 5), and the time interval $\tau = 9.07E - 4$. For different pulse shapes, the EPP number is the accumulation of the EPPs created by the six pulses. As s increases, the number of the EPPs created under each pulse increases, and the final number of the EPPs increases as well. This is due to the fact that there are more higher energy Fourier components under steeper super-Gaussian pulse, thus contributing to the creation rate of the EPPs. In addition, it was found in previous studies that the steeper the falling edge of the pulse, the smaller the annihilation rate of the particles [10]. Therefore, more EPPs are created under steeper super-Gaussian pulses (i.e. larger s), then the final EPP number is also large under the field composed of steeper super-Gaussian pulses.

We further study the dependence of the final EPP number on time interval under different pulse numbers and pulse shapes. As shown in Fig. 6, for different pulse numbers and pulse shapes, the peaks of the $N(\tau)$ curves correspond to the same time interval. Moreover, at the same time interval, the steeper the super-Gaussian pulse and the more pulses, the number of the EPPs can be significantly enhanced, e.g., the black curve under the field composed by six super-Gaussian pulses ($s = 5$). Therefore, in the study of the EPPs created in the multi-pulse field, we can choose an appropriate time interval based on the resonance expression obtained in the previous section. Subsequently, to study the enhancement effect of the multi-pulse field on EPP creation, the ratio of the final EPP number created in the multi-pulse field to that created in a single pulse is calculated. The dependence of the ratio with the number of the pulse is shown in Fig. 7.

As shown in Fig. 7, the horizontal axis represents the number of the pulses, which is denoted by M. The vertical axis is the ratio $R = N_M/N_1$, where N_M is the final number of the EPPs created in the multi-pulse field, and N_1 is the final number of the EPPs created in a single pulse, which constitutes the multi-pulse field. The time intervals $\tau = 7.75E - 5$ and $\tau = 1.5E - 4$ are corresponding to the first peak and first valley in the $N(\tau)$ curve in Fig. 6, respectively. The gray dashed line $R = M$ in the figure indicates that the pair number growth factor is equal to the number of pulses. When $\tau = 7.75E - 5$, the ratio under each multi-pulse field is greater than the number of the pulses, especially when the number of pulses is 6, the ratio approaches 14. However, when $\tau = 1.5E - 4$, the ratio under each multi-pulse field is smaller than the number of the pulses, e.g., the ratio is around 2 when $M = 6$. This is because $\tau = 7.75E - 5$ satisfies the

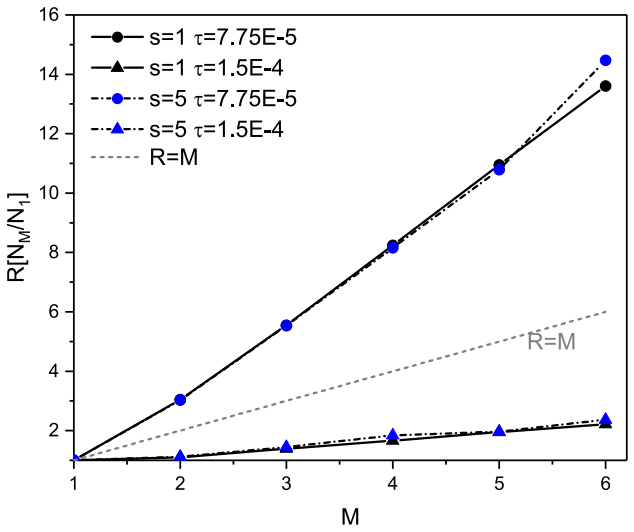

Fig. 7 The dependence of the ratio on the pulse number among the multi-pulse field. The parameters $V = 1.5c^2$, $W = 3/c$, the pulse duration $T = 1/\sqrt{2}c^2$

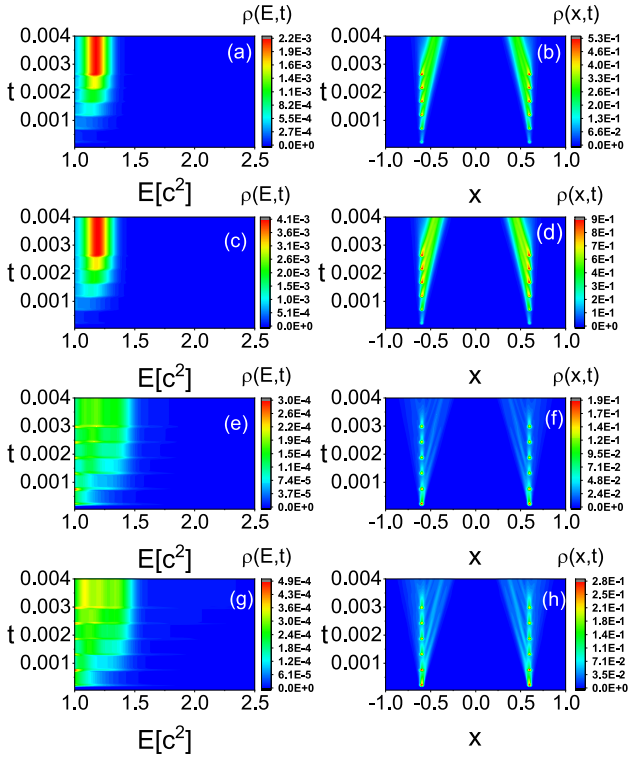

Fig. 8 The time evolution of the energy spectra and spatial distribution of the created electrons. The parameters for the eight subfigures are as follows: $s = 1\ \tau = 7.75E-5$ for (**a**) and (**b**), $s = 5\ \tau = 7.75E-5$ for (**c**) and (**d**), $s = 1\ \tau = 1.5E-4$ for (**e**) and (**f**), $s = 5\ \tau = 1.5E-4$ for (**g**) and (**h**). Other parameters $V = 1.5c^2$, $W = 3/c$, the pulse duration $T = 1/\sqrt{2}c^2$

pulse resonance condition, and the pulse resonance can significantly increase the creation of the EPPs. In addition, when $s = 5$, R is slightly larger than that of $s = 1$. Therefore, by selecting optimal time-interval, steeper super-Gaussian pulse and more pulses, the number of the EPPs will be much larger. Finally, to see more details of the EPP creation, we study the time evolution of the energy spectra and spatial distribution of the electrons.

As shown in Fig. 8, the first column is the energy spectra and the second column is the spatial distribution, with each row corresponding to the same multi-pulse field. When $\tau = 7.75E-5$, the energy spectra is narrow and gradually gathers around $E = 1.2c^2$ over time, and particles gather in the middle in the spatial distribution. When $\tau = 1.5E-4$, the energy spectra distribution is relatively wide, and the spatial distribution is relatively scattered. The temporal evolution of energy spectra and spatial distribution provides more details on the EPP creation, new particles are sequentially created under the action of six pulses, and the energy density and spatial density of electrons gradually accumulate.

4 Conclusion and outlook

In summary, we study the creation of the EPPs under the equal-sign multi-pulse field, on which there is a very little researches. The details of the EPP creation are studied from three aspects: the time evolution of the EPP number, the energy spectra and the spatial distribution of the electrons. The time evolution of the EPP number indicate that the number of the EPPs varies sequentially with the action of each pulse, and the final EPP number is the non-linear accumulation of the EPPs created by each pulse. The accumulation of the electron density is reflected by the energy spectra and spatial distribution.

Meanwhile, the dependence of the accumulation effect on the time interval, pulse shape and pulse number are studied. The time evolution of the EPP number indicates that the number of the EPPs increases significantly in a stepwise manner at better time intervals, which fulfils the pulse resonance condition. The formula for the pulse resonance condition is calculated by the perturbation method and verified by the fitting formula. Based on the formula ($\omega\tau + 2t_1\omega = 2k\pi (k = 0, 1, 2, 3...)$), suitable time interval can be selected and bad time intervals can be avoided. Besides, the accumulation effect also depends on the shape and number of the pulses. The larger the steepness of the pulses, the more number of the pulses, the creation of the EPPs can be enhanced. Finally, we find that under optimal field parameters, the number of the EPPs created in the multipule field is much greater than the sum of the EPPs created by the same number of single pulses. This not only enhance the EPP creation, but also improves pulse utilization. Due to the rapid development of the laser technology in recent years, ultra-short and ultra-strong pulses will be a powerful

tool for directly detecting the creation of the EPPs in vacuum by experiments in the future. Our findings on the EPP creation under multi-pulse field will have some guiding role for future experimental research on the EPP creation.

Funding This work is supported by the National Natural Science Foundation of China under Grant Nos. 12204001 and 11974419.

Data Availability Statement This manuscript has no associated data. [Authors' comment: All data are included in this manuscript.]

Code Availability Statement This manuscript has no associated code/software. [Authors' comment: Code/Sotware sharing not applicable to this article as no code/software was generated or analysed during the current study.]

References

1. J. Schwinger, Phys. Rev. **82**, 664 (1951)
2. J.W. Yoon, Y.G. Kim, I.W. Choi, J.H. Sung, H.W. Lee, S. KuLee, C.H. Nam, Phys. Rev. **8**, 630–635 (2021)
3. K. Krajewska, J.Z. Kamiński, Phys. Rev. A **86**, 052104 (2012)
4. A.I. Titov, H. Takabe, B. Kämpfer, A. Hosaka, Phys. Rev. Lett. **108**, 240406 (2012)
5. A. Di Piazza, Phys. Rev. Lett. **117**, 213201 (2016)
6. F. Hebenstreit, R. Alkofer, G.V. Dunne et al., Phys. Rev. Lett. **102**, 150404 (2009)
7. C.K. Dumlu, Phys. Rev. D **82**, 045007 (2010)
8. N. Abdukerim, Phys. Lett. B **726**, 820 (2013)
9. F. Fillion-Gourdeau, F. Hebenstreit, D. Gagnon et al., Phys. Rev. D **96**, 016012 (2017)
10. X.X. Zhou, C.K. Li, M. Jiang, N.S. Lin, Y.J. Li, EPL **128**, 10001 (2019)
11. S. Tang, B. King, Phys. Rev. D **104**, 096019 (2021)
12. R. Schützhold, H. Gies, G. Dunne, Phys. Rev. Lett. **101**, 130404 (2008)
13. C. Schneider, R. Schützhold, Phys. Rev. D **94**, 085015 (2016)
14. G. Torgrimsson, C. Schneider, J. Oertel, R. Schützhold, J. High Energy Phys. **06**, 043 (2017)
15. M.J.A. Jansen, C. Müller, Phys. Lett. B **766**, 71 (2017)
16. L.F. Granz, O. Mathiak, S. Villalba-Chávez, C. Müller, Phys. Lett. B **793**, 85–89 (2019)
17. X.X. Zhou, C.K. Li, N.S. Lin, Y.J. Li, Phys. Rev. A **103**, 012229 (2021)
18. R.J. Shalloo, L. Corner, C. Arran, J. Cowley, G. Cheung, C. Thornton, R. Walczak, S.M. Hooker, Nucl. Instrum. Methods A **829**, 383–385 (2016)
19. Q.L. Tian, H.X. Xu, Y. Wang, Y. Liang, Y. Tan, X.N. Ning, L.X. Yan, Y.C. Du, R.K. Li, J.F. Hua, W.H. Huang, C.X. Tang, Opt. Express **29**, 9624–9634 (2021)
20. W. Yang, S.Q. Gong, R.X. Li, Z.Z. Xu, Phys. Rev. A **74**, 013407 (2006)
21. B. Li, X.J. Jiang, X.L. Li, W.H. Hai, Y.Z. Wang, Chin. Phys. B **28**, 100303 (2019)
22. Z.L. Li, D. Lu, B.S. Xie, Phys. Rev. D **89**, 093011 (2014)
23. Z.L. Li, D. Lu, B.S. Xie, Phys. Rev. D **89**, 067701 (2014)
24. C. Kohlfürst, (2012). arXiv:1212.0880
25. B. Thaller, *The Dirac Equation* (Springer, Berlin, 1992)
26. K.D. Lamb, C.C. Gerry, Q. Su, R. Grobe, Phys. Rev. A **75**, 013425 (2007)
27. J.W. Braun, Q. Su, R. Grobe, Phys. Rev. A **59**, 604 (1999)
28. T. Cheng, M.R. Ware, Q. Su, R. Grobe, Phys. Rev. A **80**, 062105 (2009)
29. T. Cheng, Q. Su, R. Grobe, Contemp. Phys. **51**, 315 (2010)
30. see Eq.(9.9) in chapter 9, W. Greiner, B. Müller, J. Rafelski, *Quantum Electrodynamics of Strong Fields* (Springer, Berlin, 1985)
31. For a review see, e.g. and S.S. Schweber, *An Introduction to Relativistic Quantum Field Theory* (Harper & Row, New York, 1962)
32. A.D. Bandrauk, H. Shen, J. Phys. A **27**, 7147 (1994)
33. G.R. Mocken, C.H. Keitel, Comput. Phys. Commun. **178**, 868 (2008)
34. M. Ruf, H. Bauke, C.H. Keitel, J. Comput. Phys. **228**, 9092 (2009)
35. F. Sauter, Z. Phys. **69**, 742 (1931)